ELSEVIER

Journal of Power Sources 96 (2001) 133–139

JOURNAL OF POWER SOURCES

www.elsevier.com/locate/jpowsour

High-rate capability of zinc anodes in alkaline primary cells

Jean-Yves Huot*, Martin Malservisi

Noranda Inc. — Technology Centre, 240 Hymus Bvld, Pointe-Claire, Que., Canada H9R 1G5

Abstract

This work is devoted to the electrochemical aspects of high-power testing of primary alkaline LR6 (''AA'') cells and to the factors influencing cell performance, namely the corresponding zinc anode behaviour under such high-rate conditions. The influence of the high-rate testing regime, such as the discharge mode and the end-potential, on zinc utilisation in alkaline cells has been monitored and its behaviour has been isolated by means of a pseudo-reference electrode.

As anticipated, anode formulation, including zinc alloy composition and size distribution, is found to affect the cell's discharge curve and the corresponding zinc electrode potential and utilisation. The effects of these parameters on the discharge curve are discussed in terms of three stages of discharge.

Finally, the high-rate capability of commercial LR6 cells is analysed in terms of zinc anode formulation. It was concluded that zinc electrode polarisation is very small and is relatively independent of manufacturer, of zinc anode formulation and of zinc alloying. On the other hand, metallic zinc utilisation remains very low under high-rate conditions.

Keywords: Zinc-alkaline primary cells; Zinc anodes

1. Introduction

Although aqueous and non-aqueous rechargeable battery markets have been growing very fast, the primary alkaline manganese (PAM) cell remains widely used in an impressive variety of applications and devices. Small sizes, such as LR6 (''AA'') and LR03 (''AAA'') alkaline cells, even demonstrated consistent growth over the past decade as a result of continuous improvement of their overall cell performance, namely their high-rate or high-power capability. This gain is closely related to major improvements in cell components and engineering, which resulted in lower cell impedance and improved active material utilisation.

High-performance and standard commercial PAM cells have been tested under various discharge conditions. Takei et al. [1] found a significant difference between commercial cells of different manufacturers for a continuous 1 A discharge. This difference was found to vanish at low discharge currents and higher temperatures [2]. Unfortunately, the potential–time discharge curves do not provide any insight into the electrochemical behaviour of zinc anodes. Modelling of cylindrical alkaline cells showed that cell performance under high discharge rates cannot be understood without modelling the zinc anode and by taking into account anode porosity, KOH concentration, zincate ion distribution and (un)confinement to anode [3]. Previous out-of-cell anodic discharge capacities of gelled zinc alloy in electrochemical cell also showed the strong influence of zinc powder parameters on anode performance, namely the chemical composition and the presence of fine zinc particles [4].

The primary focus of this paper is to investigate the electrochemical aspects of high-power testing and factors influencing PAM cell performance, namely the corresponding zinc anode behaviour under high-rate conditions.

2. Experimental

Commercial and experimental LR6 alkaline cells were tested at room temperature and under controlled humidity with a Maccor Battery tester, System Series 4000. The cells were tested in triplicate.

Unless otherwise mentioned, commercial cells were purchased in 2000, with expiration dates after 2004. Experimental cells were half-cells supplied by a battery company, and filled with gelled zinc anode material containing a 2:1 ratio of zinc powder and alkaline solution mixed to 0.6 wt.% Carbopol 940. The alkaline solution was 40 wt.% KOH (Fisher SP236) containing 3 wt.% ZnO (Baker). Each experimental LR6 cell contained about 5.4 g of gelled zinc, or 3.6 g of zinc powder.

* Corresponding author.
E-mail address: jean-yves.huot@ntc.noranda.com (J.-Y. Huot).

0378-7753/01/$ – see front matter
PII: S0378-7753(01)00496-7

Unless otherwise mentioned, one pseudo-reference zinc electrode was inserted in the first layer of a multi-layer separator of a few LR6 cells, and both total potential and zinc potential with respect to this pseudo-reference zinc electrode were then recorded during cell discharge. In some cases, a second pseudo-reference electrode was inserted into the second layer of the separator. Cell component impedance was measured with a Solartron 1286 potentiostat and a 1260 frequency analyser.

Zinc alloy powders were made by gas atomisation of 99.995% molten zinc. Five alloys were tested, pure zinc, Bi–Zn, Bi–In–Zn, Bi–Al–Zn, and Al–Bi–In (ABI).

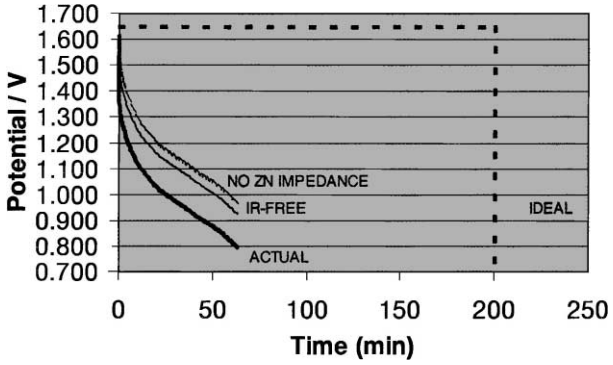

Fig. 1. Ideal and actual discharge curves of LR6 alkaline cells, and effects of cell impedance and electrochemical zinc impedance.

3. Results

3.1. The high-rate discharge of alkaline LR6 cells

Cell discharge is associated with a cell impedance that consumes part of the cell energy and induces cell polarisation which decreases cell potential. Cell polarisation consists of activation/concentration polarisation of zinc anode, activation/concentration polarisation of MnO_2 cathode, and IR loss in cell components such as electrodes, separator, and current collectors [5].

The contribution of cell components to the limited capacity and material utilisation of alkaline cells cannot be extracted from the overall discharge curve unless cell component potential and impedance are monitored as well. This was achieved by monitoring impedance and potential with respect to two reference zinc electrodes inserted in different layers of the separator. Cell impedance was measured from high to low frequencies, and ohmic contribution of cells and cell components was estimated at high frequencies, while electrochemical impedance associated with cell reaction or zinc oxidation was computed at the low end of the Z''–Z' semi-circle (Bode plot). The contribution of mass transfer was not taken into account. These results are summarised in Table 1.

The ohmic loss in alkaline cells at 1 A (R_{cell}) increases from 100 mV to 200 mV with increasing depth of discharge or decreasing cell potential, while the main contributors remain the increasing ohmic loss in active materials (R_{Zn} and R_{MnO_2}). On the other hand, the electrochemical factor is quite stable with increasing depth of discharge, and remains lower than the ohmic factor. The consistency of the electrochemical part means that the activation overpotential remains constant with increasing depth of discharge.

The impact of these factors is illustrated in the Fig. 1, wherein an actual discharge at 1 A is compared to the ideal cell discharge computed without any polarisation and ohmic loss. The ideal cell would provide about 5.5 Wh of energy per LR6 cell containing about 4 g of zinc, while the actual cell will deliver much less, with a material utilisation reaching 25% at 1 A continuous discharge. The absence of ohmic loss would actually double the energy output at the end-point potential of 1.0 V, while the absence of zinc overpotential (activation) would not significantly improve overall cell performance. The remaining gap between corrected and ideal cell potential curves can therefore be attributed to MnO_2 discharge and mass transfer in zinc and MnO_2 electrodes. Further reduction in cell polarisation will therefore not improve cell performance if the active materials utilisation remains low. It should be noted that increasing ohmic loss can be hardly distinguished from chemical passivation near the end-point potential of 0.9 V.

3.2. High-rate testing of commercial cells

The cell and zinc potentials of commercial North-American (NA1 through 3) LR6 cells were monitored during continuous discharge at 1 A. Fig. 2 shows that the discharge curves of the three brands are quite similar and much better

Table 1
Impedance of LR6 cell components at various end-point potentials[a]

Cell-potential (V)	Ohmic resistance				Electrochemical impedance	
	R_{cell}	R_{Zn}	R_{sep}	R_{MnO_2}	R_{cell}	R_{Zn}
Open circuit	0.106	0.032	0.018	0.054	0.048	0.036
1.2	0.117	0.021	0.018	0.060	0.053	0.019
1.0	0.100	0.028	0.024	0.083	0.042	0.035
0.9	0.131	0.048	0.018	0.068	0.061	0.043
0.6	0.180	0.048	Small	0.110	0.071	0.014

[a] Note: ''Sep'' stands for separator.

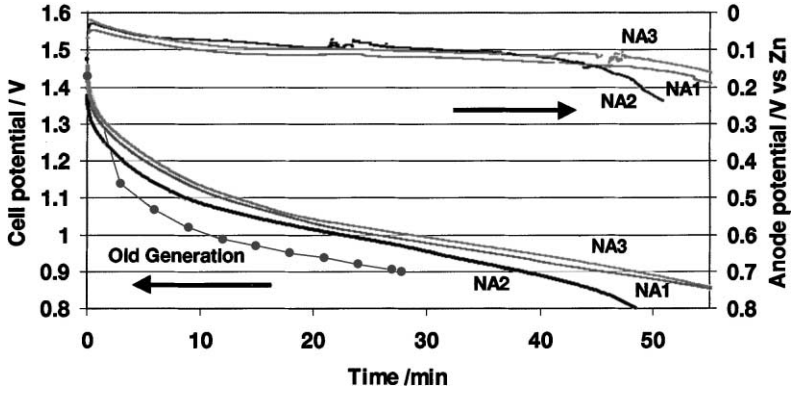

Fig. 2. Cell potentials and zinc potentials with respect to the pseudo-reference zinc electrode monitored during the continuous discharge at 1 A of commercial LR6 cells.

than the old PAM generation that was tested in 1998. Cell potential drops by about 500 mV over the entire discharge curve, while zinc anodic potential remains relatively flat at about 100 mV until cell potential reaches the end-point potential of 0.9 V. From the previous section, it can be stated that 50% of zinc polarisation is due to ohmic loss, while the other 50% is associated with the electrochemical oxidation of zinc in the early stage of the discharge.

The performance of these LR6 cells is cathode-limited as zinc potential does not drop simultaneously with the cell potential. NA2 cell performance was however found to be slightly lower than the others, while its zinc potential was quite similar to others up to 45 min, when it suddenly drops. This behaviour suggests that the NA2 zinc anode performs slightly less than NA1 and NA3, which are clearly cathode-limited. The lower performance of NA2 is much more apparent at 1 Ω and much less apparent at 1 W (Fig. 3). This is likely to be related to the initial discharge current that decreases in this order: $1\,\Omega > 1\,A > 1\,W$, as the latter corresponds to a mid-rate discharge. On the other hand, it was well established that the constant load discharge is the least severe discharge mode, if performed at the same starting discharge current, when compared to constant current and constant power [6].

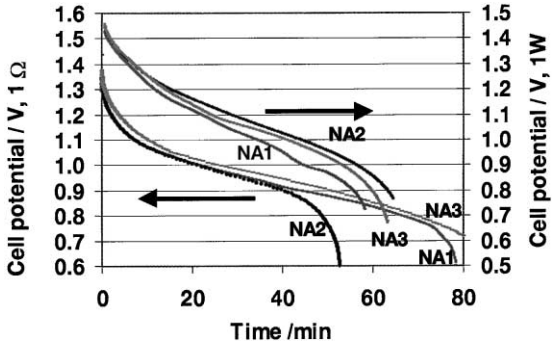

Fig. 3. Discharge profile of commercial LR6 cells under two continuous discharge modes, 1 Ω and 1 W.

As anticipated from previous work [7], the first part of both the cell and zinc discharge curves is found to follow a basic potential–time E–$t^{1/2}$ function. This function for cell and zinc suggests some similar time dependence for the cathode that has actually been reported by Laig-Hörstebrock [8]. Table 2 shows that this slope depends upon both the discharge conditions and, to a lesser extent, the cell manufacturer. The zinc electrode contributes about 3 mV $s^{-1/2}$ or 25% of cell potential drift, in perfect agreement with the extrapolated value of 3 mV $s^{-1/2}$ at 250 mA g^{-1} for gelled zinc electrodes in electrochemical cells [9].

It appears that zinc electrode polarisation consumes about 100 mV. This begins in the first part of the zinc discharge curve, while zinc utilisation in commercial anodes is established in the third part of the zinc discharge curve and would hardly exceed 25% at 1 A, or about 250 mA g^{-1} Zn. This result is in fairly good agreement with the alkaline cell discharge modelling that showed a similar zinc anode overpotential and a separator ohmic loss of about 100 mV each [6]. The actual cell potential curvature can therefore be largely attributed to the S-shaped discharge curve of MnO_2 due to the homogeneous-phase discharge which generates an S-shaped open-circuit potential versus Mn(III)/Mn(IV) ratio [10].

3.3. The electrochemical aspects of high-rate discharges

A Ragone plot of commercial LR6 cells is illustrated for three end-point potentials in Fig. 4. The energy output drops

Table 2
Initial E–$t^{1/2}$ slope of discharge curve for three commercial LR6 cells

Cell	Slope E vs. $t^{1/2}$ vs. discharge mode (V $s^{-1/2}$)			
	Zn anode at 1 A	1 A	1 Ω	1 W
NA1	0.0031	−0.0134	−0.0158	−0.0114
NA2	0.0031	−0.0114	−0.0118	−0.0093
NA3	0.0034	−0.0114	−0.0110	−0.0095

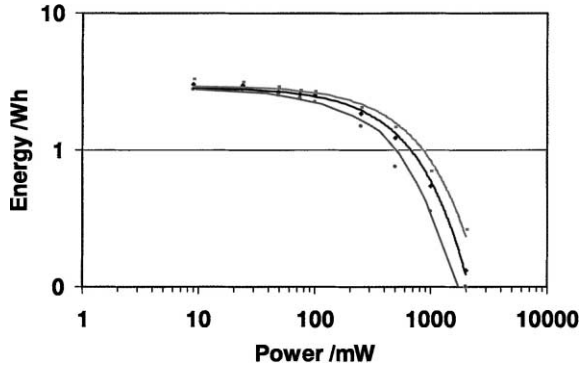

Fig. 4. Ragone plot of commercial LR6 cells for three end-point potentials.

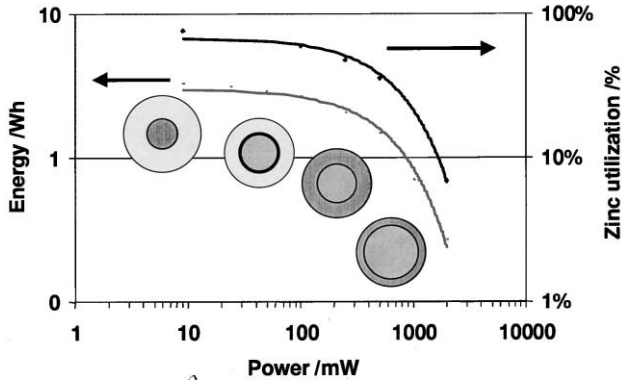

Fig. 5. Modified Ragone plot of commercial LR6 cells. A schematic cross-section of a discharged zinc anode is superimposed on the curves.

drastically when cell power reaches 0.5 W. As anticipated, this drop is more severe with increasing end-point potential.

In the Fig. 5, zinc utilisation and energy are plotted in a modified Ragone plot of commercial alkaline cells, where a schematic of the discharged anode at the end-point potential of 0.9 V is superimposed on energy and zinc utilisation curves. Schematics were drawn from color pictures of zinc cross-sections obtained from cut open cells which had been discharged down to 0.9 V. Basically, we can identify three types of zinc, gray-fresh zinc, blueish discharged zinc, and white-very discharged zinc. After high-rate discharge at 2 W, a very thin disk layer of blueish zinc precipitate is observed near the anode-separator interface, as reported for dissected discharged cells [3,11], while undischarged gray zinc is easily observed in the bulk of the anode. A Raman spectroscopy showed that blue coloration is due to ZnO [11]. The blue-discharged area expanded with decreasing power down to 100 mW, while a white-very discharged layer started forming within the blue-discharged zinc. This suggests that some deeper discharge of zinc and increased zinc utilisation are associated with the lower power. The center area remains undischarged until the extremely low power of 10 mW is reached, at which point zinc utilisation reached almost 100%.

Modelling of cylindrical alkaline LR6 cells demonstrated that the discharge layer moves toward the current collector with increasing discharge time [12], while a higher zincate concentration near the separator and corresponding zinc oxide precipitation near or in the separator could shorten cell life at increasing discharge rates.

3.4. Zinc alloy powders

Experimental LR6 cells containing various zinc alloy powders were discharged at 1 A after ageing for 7 days at room temperature. Discharge curves of five zinc alloys are shown in Fig. 6. The discharge curves basically superimpose down to 0.9 V, when the pure zinc alloy failed prematurely.

Zinc electrode potential drops in the first 10 min of continuous discharge at 1 A, where the electrode potential follows an E–$t^{1/2}$ function. The potential of the five zinc alloys then reaches a plateau at 120–150 mV for 20 min (Fig. 7). The potential of the pure zinc electrode increases suddenly after 40 min at 1 A, and this change coincides with

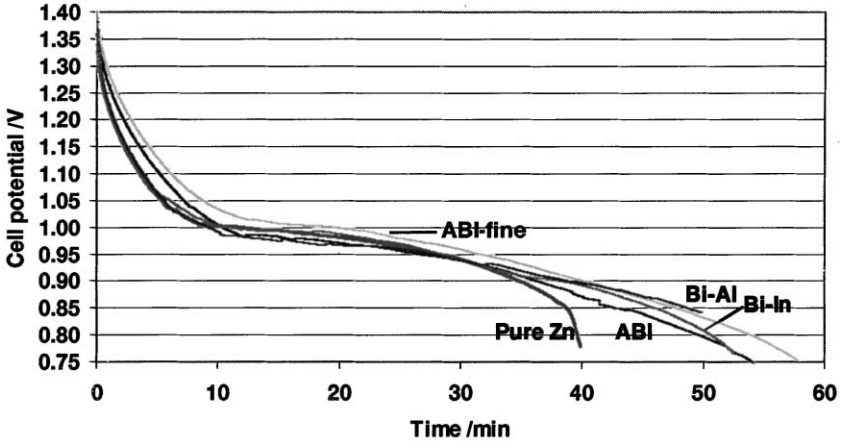

Fig. 6. Discharge curve at 1 A of LR6 cells containing various zinc alloy powders.

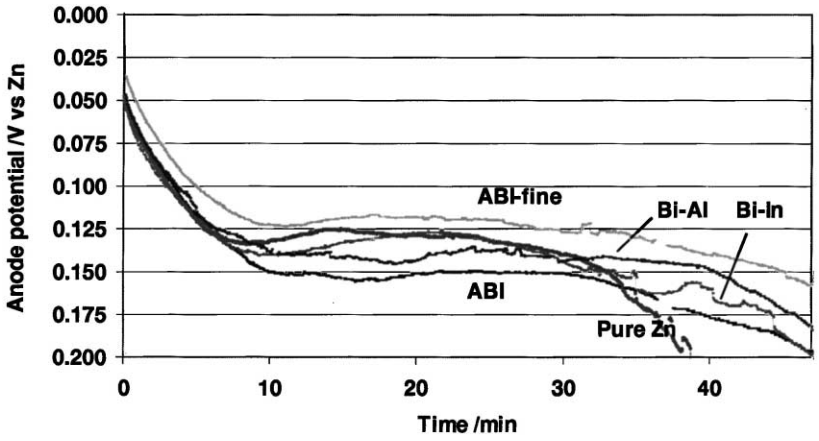

Fig. 7. Zinc electrode potentials of various alloy powders with respect to the zinc reference electrode.

the corresponding drop in cell potential. This result confirms the lower performance of pure zinc that was observed in an electrochemical cell [4]. The anodic behaviour of zinc alloy anodes suggest that pure zinc does limit cell performance, whereas cell performance is not anode-limited with the other zinc alloys, as the zinc electrode polarisation remains low when cell potential reaches the end-point potential of 0.9 V. The ultimate capacity of these zinc alloys was therefore not reached, as cell discharge was stopped as soon as the cell potential reached this end-point potential.

It can be observed that the presence of fines in the size distribution decreases zinc electrode potential by about 20 mV. This effect largely exceeds the chemical effect associated with the zinc alloys. These results are summarised in Tables 3 and 4. Again, the E–$t^{1/2}$ slope of zinc alloys accounts for about 30% of cell E–$t^{1/2}$ slope.

The anode polarisation at a given cell potential or at specific capacities remains constant for all the zinc alloys, except for pure zinc at 650 mAh. Again, these results do not tell us anything about the ultimate zinc utilisation in the cathode-limited LR6 cells.

The closed-circuit voltage (CCV) of zinc electrode contributes 30% or 50 mV to the cell CCV of 200 mV (versus open-circuit voltage (OCV)). Cell and anode resistances

Table 3
Initial slope of discharge curve and zinc anode polarisation at different depth of discharge for various zinc alloys powder

Alloy	E vs. $t^{1/2}$ slope		Anode polarisation (V vs. Zn)			
	Cell	Anode	at two cell potentials		at two capacities	
			1.2 V	0.9 V	150 mAh	650 mAh
Pure zinc	−0.0245	0.0071	0.075	0.167	0.133	0.212
Bi	−0.0203	0.0065	0.124	0.165	0.157	–
Bi–In	−0.0236	0.0066	0.087	0.159	0.139	0.157
Bi–Al	−0.0238	0.0069	0.074	0.146	0.134	0.146
ABI	−0.0163	0.0053	0.085	0.165	0.146	0.174
ABI fine	−0.0161	0.0046	0.078	0.140	0.122	0.139

Table 4
Potentials and resistances of cell and zinc anode, and in-cell after-discharge gassing (PD) of various zinc alloy powders

Zinc alloy	Zinc gassing[a] ml/3 days	Zinc anode potential			Cell potential		
		OCV vs. Zn (V)	CCV vs. Zn (V)	R_{Zn} (Ω)	OCV (V)	CCV (V)	R_{cell} (Ω)
Pure zinc	10.3	−0.006	0.048	0.054	1.609	1.408	0.201
Bi	–	−0.013	0.068	0.081	1.614	1.396	0.218
Bi–In	2.8	−0.013	0.056	0.069	1.615	1.399	0.216
Bi–Al	0.4	−0.015	0.047	0.062	1.623	1.394	0.229
ABI	0.2	−0.015	0.050	0.065	1.618	1.418	0.200
ABI fine	0.3	−0.012	0.036	0.048	1.621	1.443	0.178

[a] Discharge at 3.9 Ω/450 mAh, then 3 days at 71°C. Gassing measurement by liquid displacement.

Table 5
Zinc anode formulation and cell performance of commercial LR6 cells

Zn alloy[a]	Zn (g)	Zn (%)	D50 (μm)	OCV (V)	CCV (V)	Duration at 1 A min/s	PD[b] (μl g^{-1} day^{-1})
PI	3.1	69	316	1.587	1.135	11,09	141
BI	3.1	69	321	1.592	1.369	34,08	150
PI	3.1	65	257	1.589	1.273	19,43	660
BIC	3.6	78	248	1.603	1.283	30,24	66
BIC	3.5	76	277	1.608	1.357	36,54	178
BI	3.9	74	290	1.606	1.201	14,13	445
BI	3.7	70	288	1.597	1.173	12,52	171
AbI	3.6	68	246	1.599	1.358	38,36	1671
AbI	3.7	73	218	1.610	1.380	10,43	133
AbI	3.3	71	301	1.597	1.350	33,26	150
ABI	3.4	71	264	1.612	1.393	40,59	87
ABI	3.6	75	250	1.559	1.207	21,00	505
BIP	3.1	68	248	1.510	1.166	6,54	1000
AbI	3.3	65	309	1.583	1.310	26,59	60
PI	3.4	71	220	1.590	1.381	16,23	N.A.
ABI	3.9	71	259	1.590	1.381	19,43	N.A.
BIP	3.1	69	266	1.566	1.360	10,40	288
Pb–Zn	3.7	78	212	1.589	1.276	18,3	390

[a] P, B, I, A and C stand for lead, bismuth, indium, aluminium and calcium. The lower case b means low concentration of the alloying element.
[b] Discharge at 1 A/0.75 V, then 24 h at 71°C. Gassing measurement by liquid displacement.

were calculated from (OCV–CCV)/I and these resistances were found to be independent of zinc alloys. Anode resistance accounts for about 30% of the whole cell resistance. These resistances agree quite well with the total ohmic and electrochemical resistances measured by impedance and presented in Table 1.

As anticipated from previous out-of cell gassing evaluations [7], after-discharge gassing of zinc alloys increases in this order: ABI < BA < BI < Bi < pure Zn (Table 4).

3.5. Behaviour of world-wide commercial cells

The variability in zinc anode formulations and high-rate cell performance of commercial LR6 cells acquired world-wide in 1998 were monitored. The results are summarised in Table 5. It should be noted that both anode formulation and cell performance may have changed since that time.

Zinc quantity, the percentage of zinc in anodes, zinc particle size and zinc alloys, as obtained from zinc anodes, were found to vary substantially from one cell to another. CCV, discharge time at 1 A down to the end-point potential of 0.9 V, and after-discharge (PD) gassing all vary substantially as well. Substantial OCV variations are surprisingly observed, but can be explained by differences in KOH–ZnO concentrations and the corresponding effect on the reversible (thermodynamic) electrode potential. More surprisingly, PD gassing of ABI alloys is not lower than PD gassing of non-aluminium/zinc alloys.

4. Discussion

Monitoring of zinc electrode potential during cell discharge revealed that the zinc discharge curve is flat and slightly dependent on the alkaline cell manufacturer, anode formulation or zinc alloy powder. Zinc anode discharge at 1 A required an electrode polarisation ranging from 100 to 150 mV, which corresponds to an anodic zinc overpotential lower than 100 mV at about 200–250 mA g^{-1}. The ohmic loss of about 50 mV can be associated with the anodic ohmic loss due to electrolytic resistance, tortuosity in the porous electrode, and ZnO precipitation.

The effect of zinc alloying on zinc anode polarisation remains small, but zinc alloying appears to extend zinc utilisation by delaying the passivation of pure zinc that occurs when cell potential reaches 1 V.

In other words, the absence of an alloying element was found to induce premature zinc passivation, which suddenly appeared when the zinc potential reached 200 mV. The difference, evidenced in an electrochemical cell [4] between zinc utilisation of the other zinc alloys, was however not assessed as the experimental LR6 cells were cathode-limited.

Cell and zinc discharges involve three stages, an initial stage with potential–time E–$t^{1/2}$ function, a middle stage with a linear E–t function, and the final stage when the potential suddenly drops. This behaviour leads to three types of cell performance, (a) type I when the final stage is not observed with cells displaying a considerable ohmic drop, as the discharge is stopped when it reaches the end-point potential of 0.9 V, (b) type II, when the final stage is observed on the cell discharge curve whereas it is not observed with the zinc electrode if the cell is cathode-limited, (c) type III when the final stage is observed on both the cell and the zinc discharge curves, as the cell is anode-limited.

This work has shown that any reduction in ohmic drops in the separator and electrodes will improve the high-rate

performance of type I cells, while the benefits of reducing the overpotential of active materials will be very small. Separator impedance depends on layer thickness, porosity, the number of layers, and changes in the electrolyte composition associated with active material electrochemical reactions.

On the other hand, any reduction in cell impedance will result in a minor improvement of high-rate performance of type II and III cells if the active materials utilisation is not significantly improved. Parameters that affect zinc polarisation and zinc utilisation in alkaline cells still have to be identified and optimized in order to improve alkaline cell performance and to reduce the unit production cost of alkaline cells by reducing the zinc quantity in zinc anode material. Moreover, the electrochemical evaluation of high-rate discharge of the zinc anode in alkaline cells still needs to be addressed.

5. Conclusion

It has been shown that zinc electrode polarisation is very small, while it depends slightly on the cell manufacturer, zinc anode formulation and zinc alloying. The impact of size distribution of zinc alloy powders appears to be more significant. Parameters that affect zinc utilisation in alkaline cells still have to be identified and optimised in order to improve cell performance, especially when the cell is clearly anode-limited, namely in the case of zinc-air cells.

References

[1] T. Takei, T. Kurosawa, Y. Wada, T. Ohtsuka, J. Kawasaki, A. Sato, Prog. Batteries Batt. Mater. 16 (1997) 367–376.
[2] J. Matsumoto, B. Carter, A. Prater, D. Smith, J. Ross, in: Proceedings of the 39th Power Sources Conference, 12–15 June, 2000, p. 1.
[3] E.J. Podlaha, H.Y. Cheh, J. Electrochem. Soc. 141 (1994) 15.
[4] J.Y. Huot, E. Boubour, J. Power Sources 65 (1997) 81–85.
[5] D. Linden (Ed.), Handbook of Batteries, 2nd Edition, McGraw-Hill, New York, 1995.
[6] E.J. Podlaha, H.Y. Cheh, J. Electrochem. Soc. 141 (1994) 28.
[7] J.Y. Huot, in: A.J. Salkind, F.R. McLarnon, V.S. Bagotzky (Eds.), Proceedings of the Electrochemical Society on Rechargeable Zinc Batteries, Vol. 22, 1996, pp. 14–95.
[8] H. Laig-Hörstebrock, J. Electroanal. Chem. 180 (1984) 599.
[9] J.Y. Huot, in: A. Attewell, T. Keily (Eds.), Proceedings of the 18 International Power Source Symposium on Power Source, 1993, p. 177.
[10] A. Kozawa, R.A. Powers, Electrochem. Technol. 5 (11/12) 535.
[11] W.B. Cai, Q. Shi, M.F. Mansuetto, D.A. Scherson, Electrochem. Solid State Lett. 3 (2000) 319.
[12] E.J. Podlaha, H.Y. Cheh, J. Electrochem. Soc. 141 (1994) 15.